Fuel 320 (2022) 123887

Contents lists available at ScienceDirect

Fuel

journal homepage: www.elsevier.com/locate/fuel

Full Length Article

Cycle-to-cycle combustion analysis in hydrogen fumigated common-rail diesel engine

Ali Şanlı [a,*], İlker Turgut Yılmaz [b]

[a] Department of Maritime Mechanics, Piri Reis Vocational and Technical High School, Tuzla 34944, İstanbul, Turkey
[b] Department of Mechanical Engineering, Faculty of Technology, Marmara University, Göztepe 34722, İstanbul, Turkey

ARTICLE INFO

Keywords:
Hydrogen-diesel combustion
Cyclic variation
Engine load
Correlation coefficient

ABSTRACT

An experimental cycle-to-cycle analysis in multi-cylinder automotive common-rail compression ignition engine was performed to understand better the combustion in the hydrogen fuelled diesel engine. Hydrogen was fumigated in intake line at a wide-ranging from 0 lpm to 50 lpm in steps of 10 lpm. Test engine was operated at three different loads for a constant engine speed. The relative air–fuel ratios were between 1.55 and 3.31. The combustion occurred with an excess of air in all tests. Combustion data of 120 cycles were used to analyse the cyclic variations, determined by standard deviation of the cylinder pressure. Cyclic variations, coefficient of variance (CoV), standard deviation, frequency, and average value of peak combustion pressure (P_{max}), maximum pressure rise rate (PRR_{max}), indicated mean effective pressure (IMEP), mass fraction burned (MFB), and $MFB_{10\text{-}90}$ duration were analysed. Results showed that for all hydrogen addition levels, CoVs of P_{max}, IMEP and $MFB_{10\text{-}90}$ were always found below 3% at all loads, and PRR_{max} values with hydrogen operations in each cycle were under the limit of knocking combustion. Engine load was the most important factor to affect to CoV, standard deviation, and frequency of the combustion parameters. Minor cyclic variations in MFB traces were found at all engine loads and hydrogen addition levels, which agreed well with the cylinder pressure traces. Frequencies of P_{max} and IMEP were moderate in low and medium loads, but reduced in high load, and also the values of P_{max} and IMEP in high load were distributed in a wider range compared to low and medium loads. $MFB_{10\text{-}90}$ duration increased for dual-fuel modes, its frequency was decreased, and its distribution was extended with hydrogen addition. Trend of standard deviation was mostly similar to that of CoV for the studied combustion parameters. Furthermore, variations of correlation coefficient (R) among P_{max}, PRR_{max}, IMEP, and $MFB_{10\text{-}90}$ were discussed in this paper, and the highest R value was found between IMEP and P_{max}.

1. Introduction

Alternative fuels play a significant role in coping with increasing energy demand, reducing dependence on fossil fuels and producing less pollution than conventional fuels. Among the future potential alternative fuels, hydrogen has been recently using in internal combustion engines (ICEs) as an energy source due to cleaner exhaust emissions and excellent combustion characteristics. It is carbon free, leading to minor releasing of carbon-related emissions, and decreasing greenhouse gasses resulting in less global warming, ozone weakening, and acid rain. It can be used in compression ignition (CI) engines in dual-fuel mode with applying the techniques of the intake port or direct injection into the cylinder. Its combustion cannot be directly started by compression temperature owing to high self-ignition temperature; therefore, it is needed to some amount of the conventional fuel, called pilot fuel. Hydrogen extends flammable limits and can burn in leaner mixtures in dual-fuel mode [1]. It has higher laminar flame speed than that of the conventional fossil fuels. Besides, its high diffusivity decreases heterogeneity of the diesel fuel spray; hence, existing more uniform mixture and high combustion efficiency [2]. The mass calorific value of hydrogen is almost three times higher than that of the conventional diesel fuel. However, this property can encourage the formation of nitrogen oxides in the hydrogen dual-fuel mode [3]. When the engine is run with a rich mixture, problems such as knocking, pre ignition and backfire may occur [4]. Smaller quenching distance and very low ignition energy of the hydrogen can also be resulted in abnormal combustion such as the pre-ignition or knocking [5]. For the reasons, hydrogen utilization in the ICEs is limited to run at higher engine loads and speeds.

* Corresponding author.
E-mail address: phdalisanli@outlook.com (A. Şanlı).

https://doi.org/10.1016/j.fuel.2022.123887
Received 19 January 2022; Received in revised form 6 March 2022; Accepted 14 March 2022
Available online 23 March 2022

Table 1
Engine specifications.

Engine Type	In-line 4-cylinder
Fuel injection system	Common-rail direct injection with single pre-injection
Bore	7.6 cm
Stroke	8.05 cm
Compression ratio	16.9
Number of valves	8
Displacement volume	1461 cm^3
Max. power (@4000 rpm)	48 kW (65 hp)
Max. torque (@1750 rpm)	160 Nm

CI engines suffer from the vibrations which are detrimental to engine components. In order to cope with the engine vibrations, the cycle-to-cycle variations (CCVs) must be decreased as much as possible [6]. During the transient engine operations, a number of parameters and boundary conditions such as air–fuel ratio, inlet pressure and temperature, humidity, residual burnt gases, and injection features affect the cycle-to-cycle combustion behaviour [7,8]. Achieving the desired control level during transient operations is highly difficult because these variables defining the stable engine operating must be precisely maintained. The characterization of CCVs is important in many aspects especially for modern ICEs that can be run on alternative fuels. Even small changes in inlet conditions can provide uneven distribution of the air–fuel mixture in the cylinders. Diluent type, condition of charge in intake manifold during the closed period of the intake valves (hydrogen-air mixture in this study), charge motion, trapped mass, injection rate, residual gases from last cycle, ignition delay and initial flame development period may be considered as the main reasons of the CCVs [7,9,10]. Therefore, larger CCVs during the engine operation will be resulted in uneven power production of the cylinders, preventing the engine from achieving its full potential efficiency, and resulting in uncomfortable driving conditions [11,12]. Severe CCVs are also associated with formation of the carbon monoxide and unburned hydrocarbon emissions [13], as well as fuel consumption [14]. The need for more detailed investigations on CCVs is expected to better understand the combustion nature in the ICEs run on alternative fuels and to cope with the specified problems.

Many researchers studied CCVs in dual-fuel engines employed with different alternative fuels. Santoso et al. [15] experimentally studied cyclic variations in case of hydrogen utilization in a CI engine. Hydrogen was introduced into the intake manifold, and the test engine was run at various loads for a constant engine speed. They reported that peak pressure fluctuations of the main combustion increased with increasing the engine load. At low engine load, hydrogen addition caused unstable variations in the combustion pressure, and resulted in wider fluctuations in indicated mean effective pressure (IMEP). Zhou et al. investigated effect of hydrogen addition in a CI engine on emissions, cyclic variations and combustion characteristics. At low engine load and speed, coefficients of variance (CoVs) of IMEP and maximum pressure rise rate (PRR_{max}) increased due to heterogeneous nature of the air–fuel mixture,

Table 2
Relative air–fuel ratio values under different operations.

Load	H0	H10	H20	H30	H40	H50
0.34 MPa	2.94	2.74	3.31	3.26	3.13	3.25
0.69 MPa	1.99	2.14	2.17	2.15	2.16	2.17
1.03 MPa	1.57	1.58	1.57	1.55	1.58	1.55

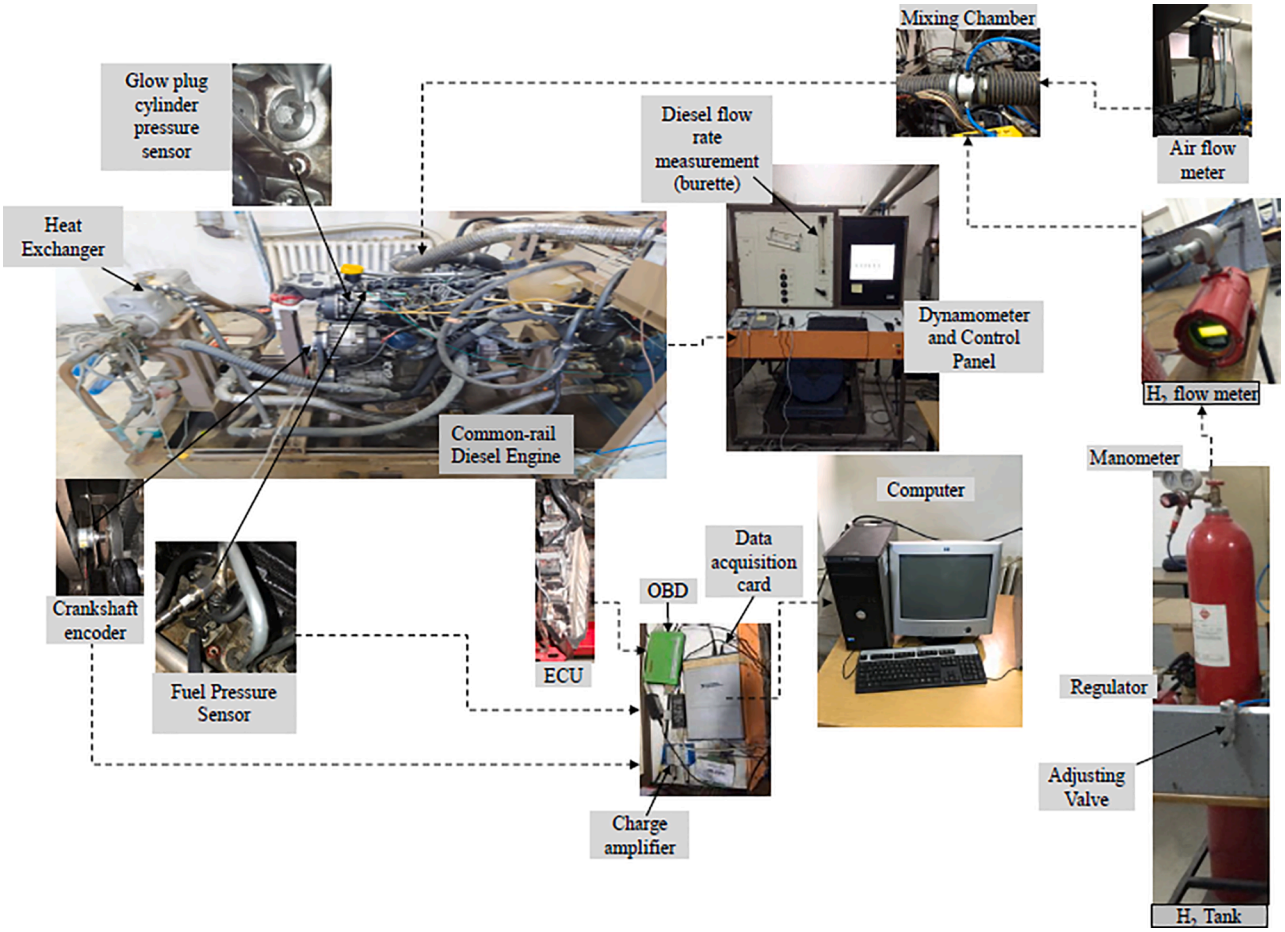

Fig. 1. Experimental test arrangement.

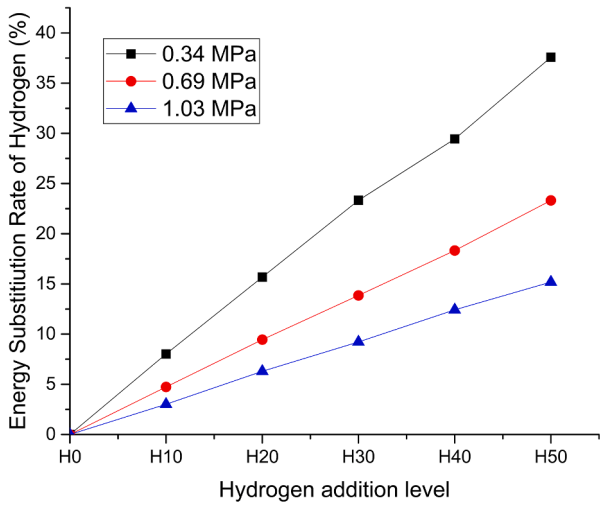

Fig. 2. ESR trends with the hydrogen addition levels at different engine loads.

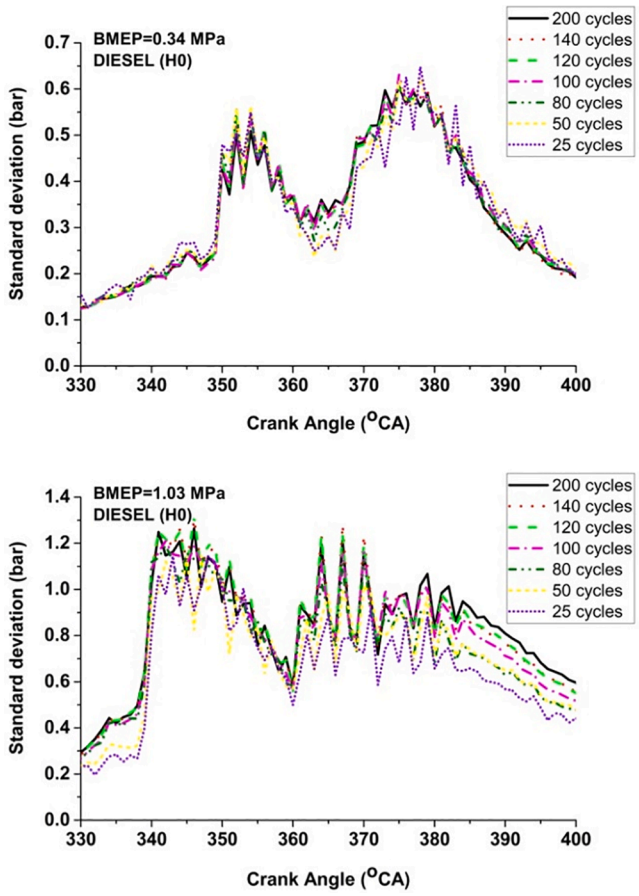

Fig. 3. The standard deviation of the combustion pressure for the various numbers of the cycles @1750 rpm.

meaning that a poor operation for an ICE was existed. At high engine load and speed, CoV of IMEP diminished, but CoV of PRR_{max} enhanced. Fast flame propagation of the hydrogen accelerated the combustion in dual-fuel mode and decreased the duration of diffusion combustion phase, providing that the combustion is more rapidly and more vigorously but it caused the knock. Jagadish and Gumtapure [6] experimentally studied cyclic variations in biogas-diesel engine. Raw biogas ratios in the mixtures were varied from 20% to 60%. Authors reported the dual-fuel engine run stable and combustion was stable with 40% biogas. Port injected dimethyl ether in premixed charge CI engine was also used to investigate CCVs. The dimethyl ether exhibited lesser CoVs of IMEP and maximum in-cylinder pressure (P_{max}) than 3% [16]. Optimized dimethyl ether proportion was found to decrease cyclic variations and to extend the operating range in a premixed charge CI engine. In a biodiesel used CI engine, Yang et al. [13] documented that biodiesel adding decreased CCVs compared to conventional diesel fuel in a CI engine at part loads. Oxygen presence in biodiesel fuel is beneficial to increase the oxidation of the fuel and shortens the ignition delay, which leads to lower cyclic fluctuations. Natural gas (NG) has a lot of properties such as high-octane number, air–fuel ratio, flammable limits, etc. which affect to cyclic combustion variables. CCV behaviours of the NG fuelled engine are dependent on proportion of the NG in the mixture. Zheng et al. [17] investigated the cyclic variations in a NG direct injection spark ignition (SI) engine with different compression ratios. They revealed that variations in flame development duration and late combustion duration were main sources of the CCVs in NG direct injected engine. Gupta and Mittal [18] investigated performance, emissions, and cyclic variations in SI engine fuelled with biogas under different compression ratios. The authors found that cycle-to-cycle variations were reduced with increase in compression ratio. P_{max} was related to PRR_{max} and location of maximum in-cylinder pressure, which were in a linear relationship; also a quadratic relationship between IMEP and location of P_{max} was found. Wang et al. [19] studied the effect of NG utilization on the cyclic variations in a CI engine. In case of moderate NG percentages, deviation rate was stable, and the cyclic variation of the mass fraction burned was highly unstable. Similarly, Jha et al. [20] investigated the effect of methane energy fraction on the CCVs in a CI engine and found significant fluctuations in the dual-fuel combustion. The cyclic variations of in-cylinder pressure increased with an increase in methane energy fraction due to a decrease in overall reactivity of the charge, since methane reactivity is less than that of the diesel fuel. In an SI engine running with NG [21], different proportions of methanol as pilot fuel generated lower CCVs in P_{max} and also lower frequency in the various cyclic parameters. The effect of water injection on cyclic variations of a NG engine at low load was investigated by Chen et al. [22]. This application was used in aircraft engines in 1930s, and the technic was then applied in ICEs in order to decrease thermal load and deal with the higher turbine inlet temperature as well as the engine knock. Regarding cyclic variations in ICEs, it was reported that the wider range of frequency distribution and remarkable fluctuations were seen in IMEP by the water injection. Besides, the CoV of IMEP increased with the increase in the amount of injected water and decreased below 3%. The hydrogen usage in NG dual-fuel SI engine was studied by the investigators [23,24], and their results gave lower CoV of IMEP and CoV of P_{max} with hydrogen addition. Maurya and Agarwal [11] studied CCVs in methanol and gasoline fuelled homogeneous charge compression ignition engine and reported that the critical parameters affecting the engine operating range were PRR_{max} and CoV of IMEP.

Analysis of the CCVs brings a large understanding about combustion stability and operating limits of the hydrogen enriched engines. As can be concluded from the literature review above, many studies have been recently conducted regarding the effects of different alternative fuels on the CCVs in CI and SI engines; however, very limited work has been found about the effect of hydrogen on the CCVs of dual-fuel CI engines. Besides, there is limited finding on the components including standard deviation and correlation coefficient for the examined cyclic parameters. The aim of the study is to investigate the CCVs of hydrogen fuelled four-cylinder common-rail CI engine.

2. Experimental study

2.1. Apparatus and procedure

A four-cylinder, turbocharged automotive common-rail CI engine

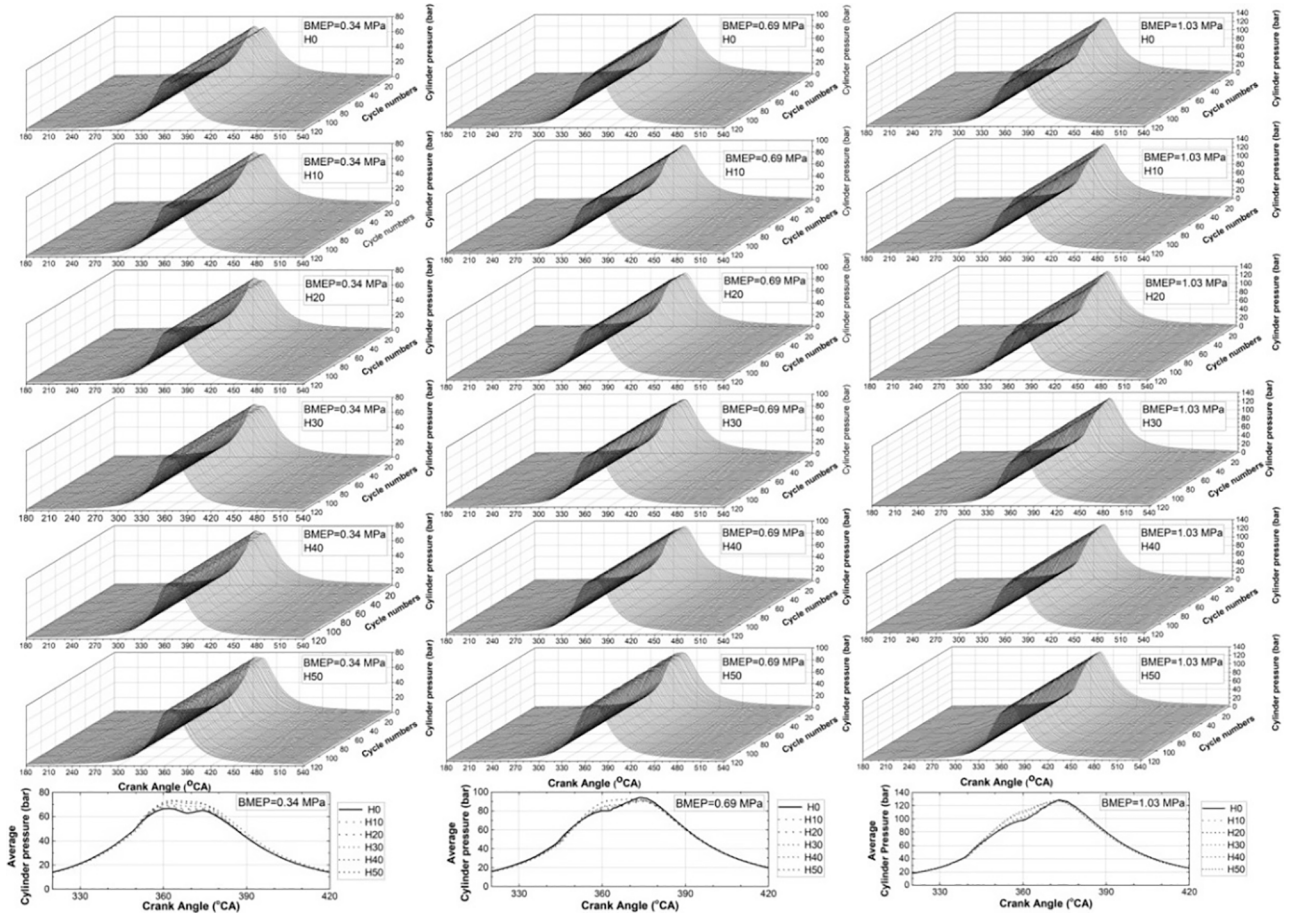

Fig. 4. Combustion pressure of the consecutive 120 cycles, and average with CA for various hydrogen fractions and BMEPs @1750 rpm.

was run for the experimental study. Key properties of the test engine are presented in Table 1, and experimental test arrangement is demonstrated in Fig. 1. The engine was coupled to an eddy-current dynamometer and was tested under three different brake mean effective pressures (BMEPs) (3.4 bar, 6.9 bar and 10.3 bar) at constant rotational speed of 1750 rpm. With K-type thermocouples, temperatures of the inlet air, exhaust gas, cooling water, lubrication oil, and diesel fuel were measured. Temperature of the cooling water was kept constant at 80–85 °C, and the coolant was cooled by a heat exchanger in which separately circulated the municipal water. The temperature of the lubrication oil was kept about 100 °C by oil cooler. Lubrication oil temperature was arranged by self-heat exchanger of the engine. Inlet air flow rate was determined via an air flow meter of New Flow brand. The diesel fuel amount flowing in glass volumetric pipe was determined with a digital chronometer. The hydrogen amount was measured through Sierra mass flow meter. All uncertainties for the used equipment can be found in earlier studies of the authors [25,26].

2.2. Combustion data collecting

Combustion pressure data was collected by a pressure sensor (Optrand, 32288) integrated in glow plug of the first cylinder. This sensor connected to fiber-optic cable directly exposes to combustion chamber and thus doesn't need to any connecting passage and besides not need a separate signal conditioner. Instant pressure variations in rail fuel line were also determined by a Kistler transducer (C6533 A11). Fuel line pressure signal was amplified by an amplifier (Kistler 4067C2000S) and sent to a data acquisition card (National Instrument, 6343). In the meantime, a crankshaft encoder (Kubler) generating 360 pulses per revolution was used to define crankshaft rotational position. Both the pressure in the first cylinder and the pressure in fuel line were filtered by software in a computer. A Bosch brand on-board diagnostics (OBD) device was used to display instantly some engine operating data including angle of the accelerator, rail pressure, boost pressure, and fuel temperature.

2.3. Fuelling procedure

In the tests it was used low sulphur diesel fuel. Hydrogen gas having purity of 99.999% in a 50 l bottle was fumigated with intake air in a mixing chamber and its pressure was decreased to 1 bar by a pressure regulator. A flame arrester was used to prevent the test system from exploding or back-pressure in the gas line. After the engine achieved to the steady-state condition, baseline diesel tests were conducted. In dual-fuel modes, the hydrogen was supplied in flow rates from 10 l per minute (lpm) (H10), to 50 lpm (H50) with increments of 10 lpm. The amount of hydrogen was adjusted by control valves. In order to reach the expected BMEP, the amount of the diesel was changed depending on the target amount of hydrogen. Moreover, lean-burn operations were maintained during the diesel-hydrogen tests. Relative air–fuel ratio values obtained at each test condition are given in Table. 2.

2.4. Calculation method

The energy substitution rate (ESR) of the hydrogen was determined by following equation.

$$ESR = \frac{\dot{m}_{hydrogen} LHV_{hydrogen}}{\dot{m}_{hydrogen} LHV_{hydrogen} + \dot{m}_{diesel} LHV_{diesel}} 100 \quad (1)$$

where; $\dot{m}$ (kg/s) symbolizes mass flow rate of the fuel, LHV (kJ/kg) is

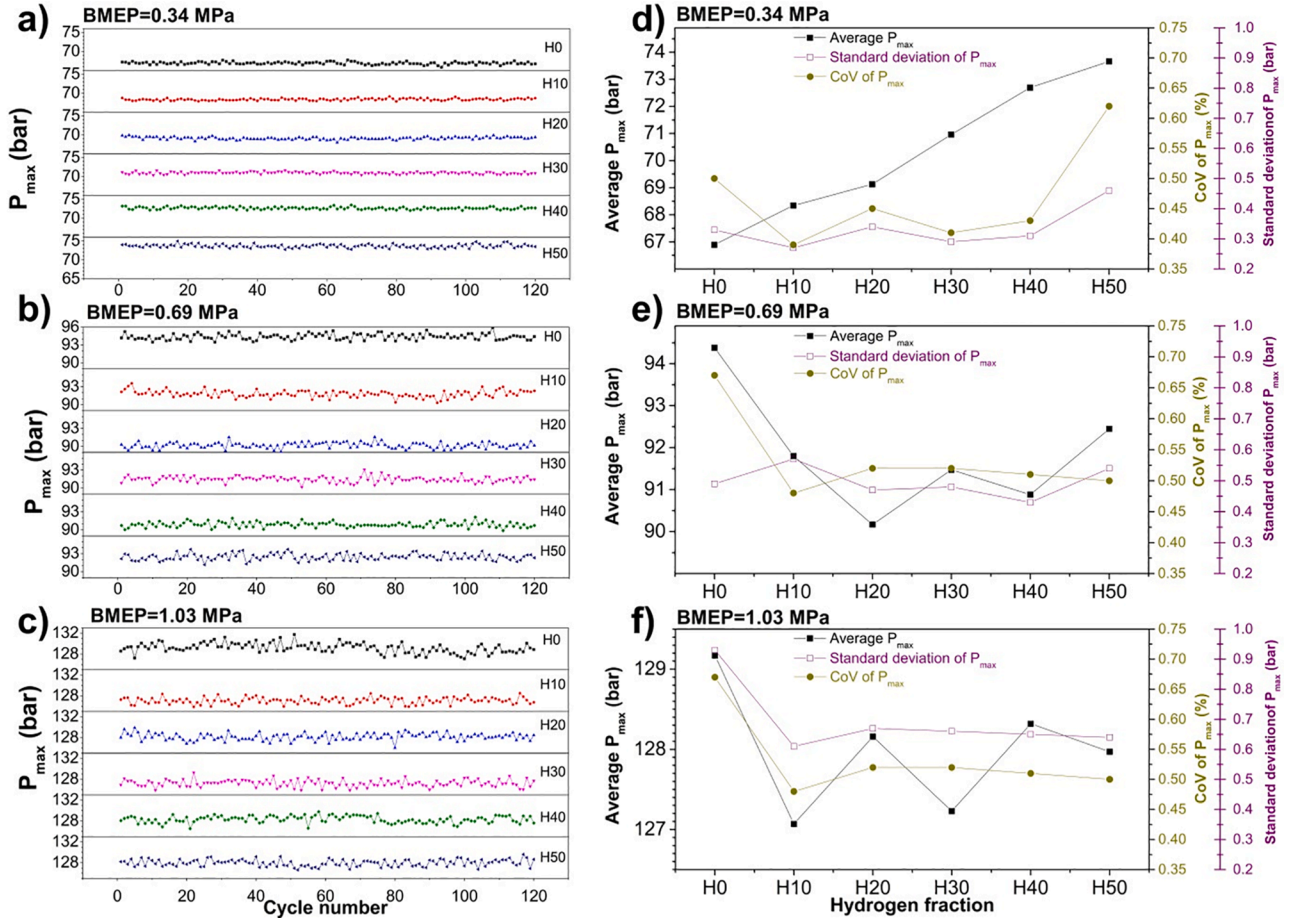

Fig. 5. Cyclic variations (a, b, and c) and average, standard deviation, and CoV (d, e, and f) of P_{max} at different hydrogen fractions and BMEPs, @1750 rpm.

Table 3
Differences in P_{max} during various working cycles.

	Lowest P_{max} (bar)			Highest P_{max} (bar)			Difference		
Hydrogen fraction	0.34 MPa	0.69 MPa	1.03 MPa	0.34 MPa	0.69 MPa	1.03 MPa	0.34 MPa	0.69 MPa	1.03 MPa
H0	65.81	93.45	127.08	67.71	95.91	131.76	1.9	2.46	4.68
H10	67.83	90.30	125.86	69.16	93.56	128.49	1.33	3.26	2.63
H20	68.01	89.11	126.04	69.92	91.57	129.88	1.91	2.46	3.84
H30	70.33	90.15	125.87	71.63	93.11	129.25	1.3	2.96	3.38
H40	72.08	89.86	126.53	73.51	92.14	129.77	1.43	2.28	3.24
H50	72.73	91.15	126.61	74.94	93.71	129.60	2.21	2.56	2.99

lower heating value of the fuel. The ESR of hydrogen can be seen in Fig. 2. Consuming more diesel fuel with increasing engine load decreased the ESR of hydrogen.

The IMEP denotes the mean in-cylinder pressure in one cycle, and it is computed by using the experimental combustion pressure (P), volume change (V), and displacement volume (V_d) by equation below [13].

$$IMEP = \frac{\sum(P_i + P_{i+1})(V_{i+1} - V_i)}{2V_d} \tag{2}$$

The CoV is coefficient of variation of a combustion sample and characterizes the degree of distribution of data from the average cycle value. It is determined from equation below.

$$CoV = \frac{\sigma}{\overline{X}}\,100 \tag{3}$$

where, σ and $\overline{X}$ respectively stand for the standard deviation and the average cycle value of a combustion sample. σ is calculated from.

$$\sigma = \sqrt{\frac{\sum_{i=1}^{n}(X_i - \overline{X})^2}{n-1}} \tag{4}$$

X_i is a random engine combustion parameter such as P_{max}, IMEP, PRR_{max} or $MFB_{10\text{-}90}$ (combustion duration). n specifies the number of cycles.

In order to determine the relationship between the studied combustion parameters, the correlation coefficient (R) is obtained by Eq. (5).

$$R(X,Y) = \frac{\frac{1}{n}\sum_{i}^{n}(X_i - \overline{X})(Y_i - \overline{Y})}{\sigma_{(X)}\sigma_{(Y)}} \tag{5}$$

In this paper, the relations between main samples containing P_{max}, PRR_{max}, IMEP, and $MFB_{10\text{-}90}$ were investigated by considering the correlation coefficients of R(P_{max}, PRR_{max}), R(P_{max}, IMEP), R(PRR_{max}, IMEP), R($MFB_{10\text{-}90}$, IMEP), R($MFB_{10\text{-}90}$, PRR_{max}), and R($MFB_{10\text{-}90}$, P_{max}).

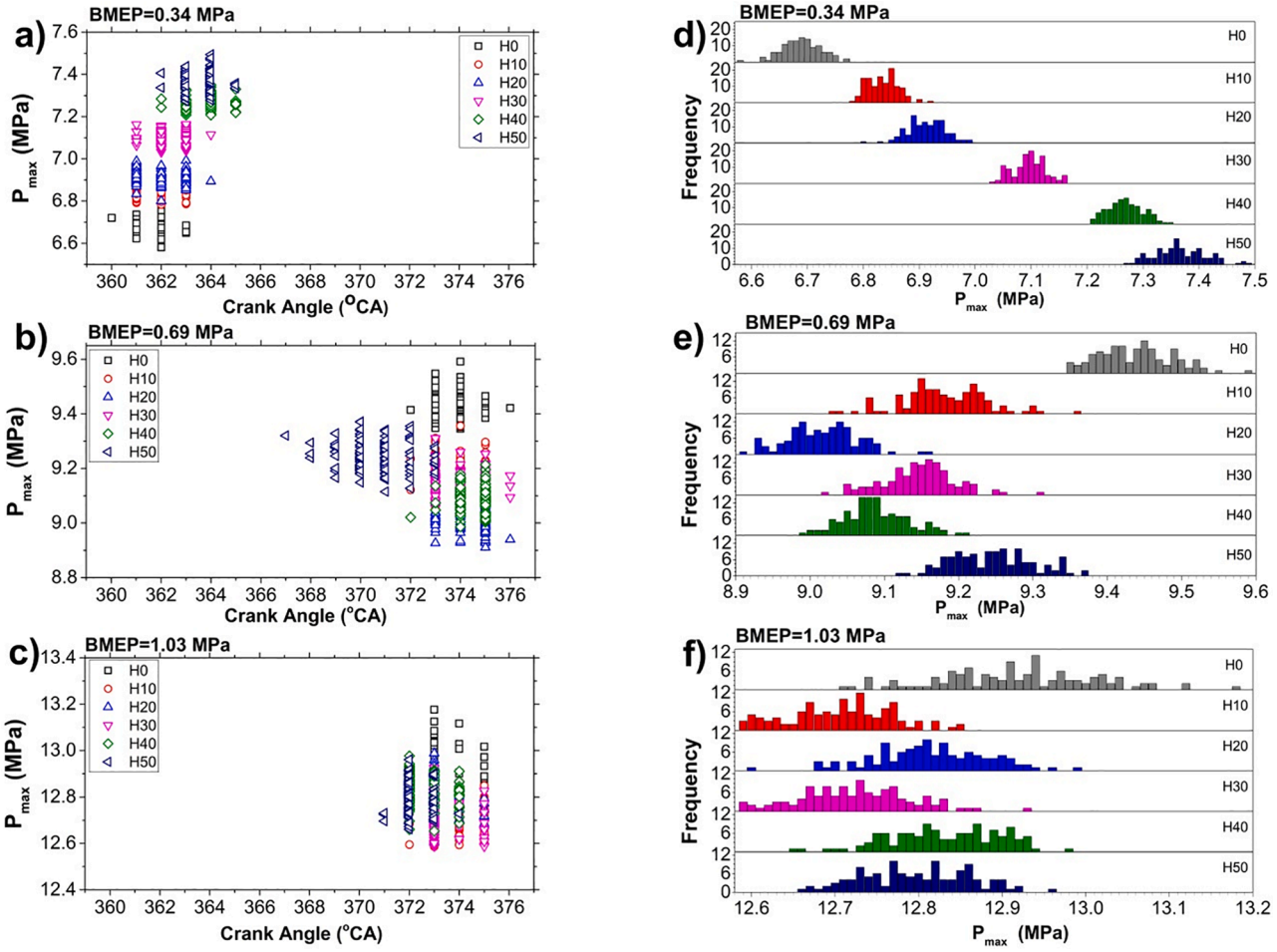

Fig. 6. Scatter diagram of P_{max} versus its crank angle, and frequency of P_{max} under various hydrogen fractions and BMEPs @1750 rpm.

3. Results and discussion

3.1. Determination of cyclic number to be studied

The standard deviation is an indicator for amount of variation of the combustion data sample. Its value indicates deviation from mean value. The number of cycles is important factor in the cyclic combustion analyses and can be determined by standard deviation. For a studied combustion parameter, the standard deviation calculated with a large number of cycles can be essentially similar to that of the standard deviations calculated with a small number of cycles. In this case, the number of cycles can be reduced by taking into account the standard deviation for the combustion sample. This is also beneficial to reduce the computation time and work-load. Cylinder pressure is the main part of cyclic combustion analyses and other combustion parameters are calculated depending on that. Fig. 3 compares the standard deviation of the combustion pressure for the low and high load tests. Standard deviation traces calculated using 120 and above cycles are very close to each other, so it is basically concluded that there is no need to study with larger cycle numbers. In this regard, cycle-to-cycle combustion findings in this paper are presented using 120 cycle data. This approach was adopted by Wang et al. for cyclic combustion analysis in NG fuelled CI engine [19].

3.2. Cyclic analysis of cylinder pressure

Fig. 4 indicates consecutive combustion pressure traces for 120 cycles and their average with crank angle (CA) at different cases. It was clearly observed that combustion pressure for each cycle was highly similar to each other in a certain condition. It meant that there was no trouble in cylinder pressure oscillation and no pre ignition, and thus provided stable combustion in operation with hydrogen dual-fuel modes. Conversely, Santoso et al. [15] reported the considerable cyclic pressure instabilities which could occur in a hydrogen-diesel combustion in comparison with the conventional diesel combustion. According to their study, peak pressure decreased with the addition of hydrogen at low load due to less energy percentage of the pilot diesel and resulted in late start of the combustion. In Fig. 4, it was observed that the combustion pressure of the hydrogen fuelled diesel engine in the compression stroke was a little less than that of the diesel fuel due to having higher specific heat content and absorbing the energy of mixture by the injected pilot diesel. After the start of combustion, peak cylinder pressure for the hydrogen enriched operations relatively increased at low BMEP; however, it reduced at medium and high BMEPs compared to single diesel operation. For the various flow rates of the hydrogen, the premixed combustion phase improves and starts moving towards earlier CA locations compared to that of the single diesel fuel operation. This is resulted in existing earlier peak pressures at especially increased engine

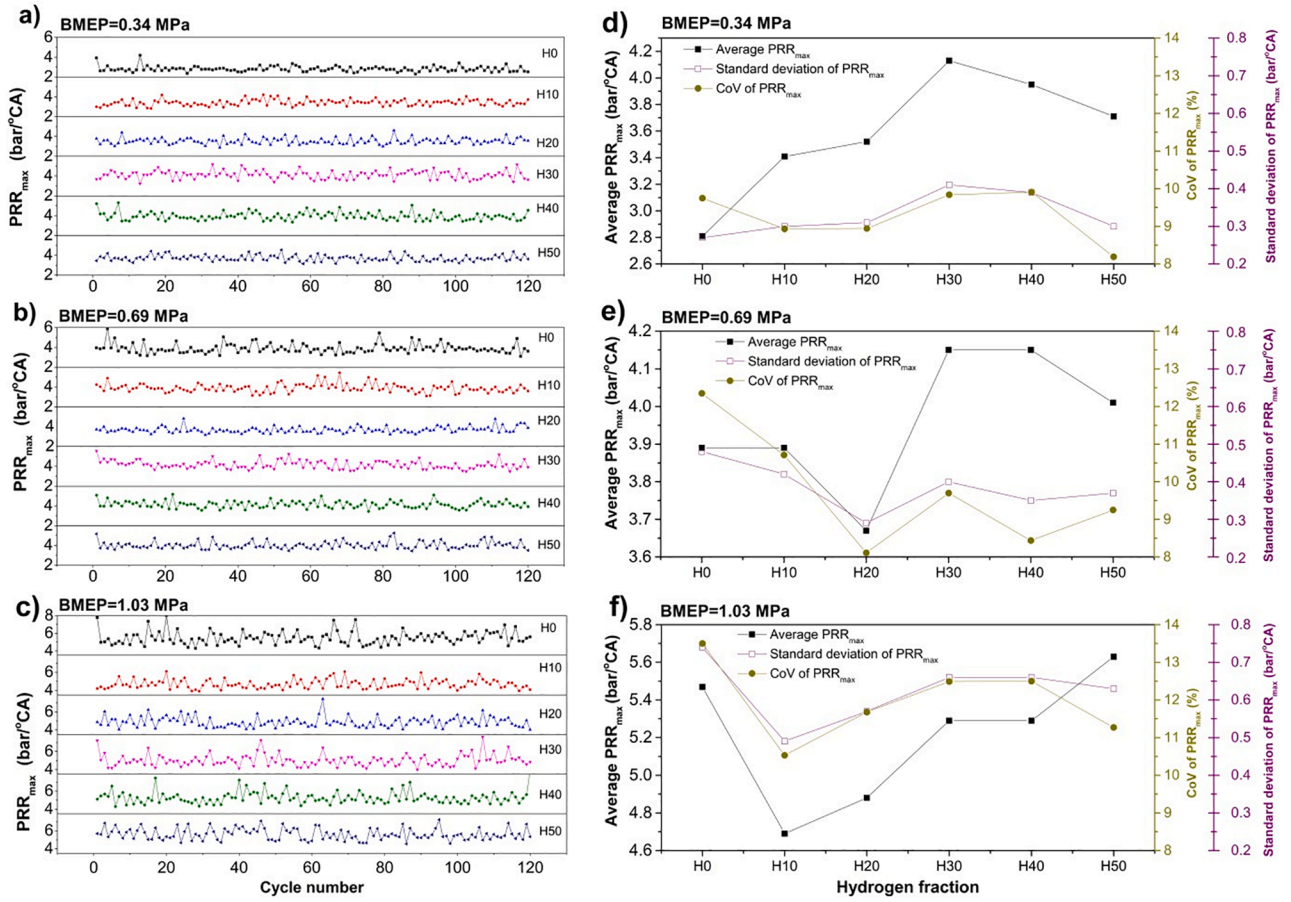

Fig. 7. The cyclic variations (a, b, and c) and average, standard deviation, and CoV (d, e, and f) of PRR_{max} at different hydrogen fractions and BMEPs @1750 rpm.

loads. At low load, the lean mixture reduces pressure and temperature of the combustion gases but some properties of the hydrogen encourage the combustion behaviour. Fast flame speed of the hydrogen might be responsible for earlier peak in-cylinder pressure. Not only increasing the pilot fuel amount but also increasing the hydrogen percentage provide strong combustion phase at rich conditions. On the other hand, they have a limited effect on earlier peak pressure occurrence. The test engine has double injection stages. The first stage is the pre-injection, and the second stage is the main injection. Therefore, two peaks were observed in the cylinder pressure traces depending on engine operating conditions. Amount, starting time, and duration of the injection dependently change with the engine load. The peak pressure magnitudes and their occurrence locations sturdily depend on the injection characteristics of the test engine [25].

Fig. 5 exhibits typical fluctuations in the values of P_{max} (a, b, and c), and CoV, standard deviation, and average value (d, e, and f) obtained in operation with the various hydrogen flow rates and BMEPs. It was observed that the values of CoV of P_{max} for all operating conditions were less than 1%, meaning that the engine was run smoothly with the hydrogen addition, which was well consistent with the consecutive cylinder pressure traces presented earlier in Fig. 4. As the hydrogen was supplemented to the intake manifold at lower flow rates at all BMEPs, the CoVs of P_{max} first decreased and then followed a weaving trend. The CoVs increased noticeably with H50 at low load since such a greater amount of hydrogen formed much concentrated air–fuel mixture. It caused a poor combustion process, and thus possibly occurring lower combustion efficiency. Consequently, higher standard deviation and CoV of P_{max} were produced. As one of the worthwhile results, CoV trend of P_{max} was almost similar to that of the standard deviation of P_{max}. Most factors could affect to the CCVs of the P_{max}. In dual-fuel modes, at low engine loads less energy basis of the pilot fuel and lower injection pressure may create poorer combustion regions. In this case the ignition cores formed in the cylinder were less due to low temperature and inefficient combustion. Moreover, the hydrogen-air homogeneity in the cylinder was not high enough to achieve efficient combustion process. On the other hand, CoV of P_{max} and standard deviation increased as the engine load was increased. Increase in total fuel amount with the enhanced loads strengthens the combustion process, which increases fuel reactivity leading to higher combustion temperature and pressure. This affects to CCVs as increasing the load [20]. Moreover, an increase in pilot diesel amount with increasing load caused an increase in the number of ignition cores in combustion chamber and existing of richer burning regions [6]. Certain uncertainties in the fuel injection stages and the ignition delay, and residual gases from the previous cycle might also contribute to CCVs [7,27–30].

Considering the standard deviation of P_{max}, it was ranged from 0.27 bar to 0.93 bar, and increased with the increase in BMEP due to more fluctuations in the combustion pressure. This could be recognized from Table 3, in which was covered the lowest and the highest values of the combustion pressure, and the difference between them in each test condition. The biggest difference was found with H50 at low BMEP, and with H10 at medium BMEP, and with single diesel fuel at high BMEP.

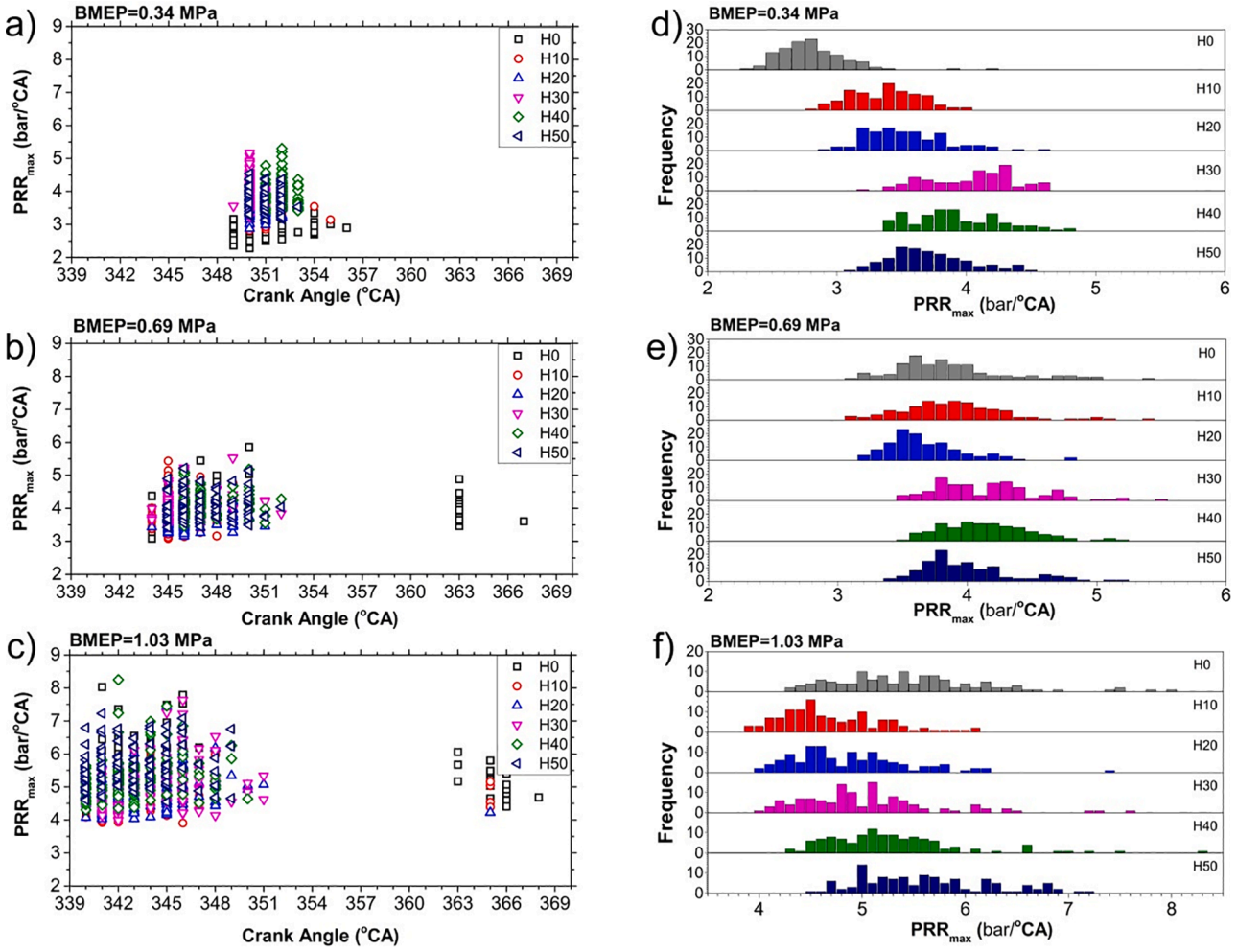

Fig. 8. Scatter diagram of PRR_{max} versus its CA, and frequency of PRR_{max} under various hydrogen fractions and BMEPs @1750 rpm.

Overall, the condition that the standard deviation of the P_{max} was the highest could be high precisely associated with the condition that the difference between maximum and minimum values of the P_{max} was the highest.

Another important cyclic relationship is between the P_{max} and its corresponding location, which will be referred as scatter diagram, in Fig. 6 (a, b, and c) for 720 data points, and between frequency (cycle number) and distribution in the values of P_{max} for the examined working cycles, in Fig. 6 (d, e, and f), under various hydrogen fractions and BMEP conditions. Engine performance is proportionally affected by magnitude and location of the P_{max}. In a reciprocating piston engine, for the best torque, peak combustion pressure should be often reached at a CA of 10-15° after top dead centre (TDC) [31]. At the same time, to ensure vigorous engine operation and comfortable driveability the peak combustion pressure patterns must follow minimal fluctuations. From the scatter diagram, it was observed that the location of the P_{max} for all fuel combinations retarded with enhanced BMEP. At low load, the pre-injection stage of the pilot diesel played a role to occur in the earlier CAs of P_{max}. With the larger addition of the hydrogen, the location of P_{max} was remarkably advanced at medium and high BMEPs due to the higher combustion rate and temperature at the richer mixture, whereas it was retarded at low BMEP. It was also noticed that these findings were consistent with earlier combustion samples on the average combustion pressure (in Fig. 4 and Fig. 5). The magnitude and occurrence location of the P_{max} depend on engine load [28,29,32]. The engine load is increased by the addition of hydrogen and pilot fuel, resulted in an increase in combustion pressure and temperature. Moreover, the hydrogen addition causes faster flame propagation in dual-fuel modes [28,33]. Consequently, P_{max} in hydrogen-diesel fuelled CI engine at high load shifted toward earlier CA locations. In addition, the pre-ignition phenomenon in the examined cycles was not noted at all in spite of the larger hydrogen amounts and BMEPs. Zhou et al. [5] reported some pre-ignition cycles in running with larger hydrogen amounts in a CI engine at high engine load and speed, resulted in quite advanced CA locations and higher P_{max} values. According to the authors, shortened ignition delay was responsible to that case. In the literature, this type of abnormal combustion cycles was found in both CI and SI engines [5,34]. The cyclic variation of the diesel combustion is known to be very regular and stable [29] due to the nature of non-premixed combustion [7]. As to the frequency of P_{max} values, it was observed that the maximum repeatability and distribution range in the values of P_{max} changed depending on BMEP and the hydrogen amount. In Fig. 6 (d), the values of P_{max} were distributed in the range of about 0.2 MPa for each hydrogen-diesel operation, and the maximum repeatability (frequency) was between 15 and 21 cycles at 0.34 MPa BMEP. When the engine was run at the highest test load, as can be seen from Fig. 6 (f), the values of P_{max} were distributed in a wider

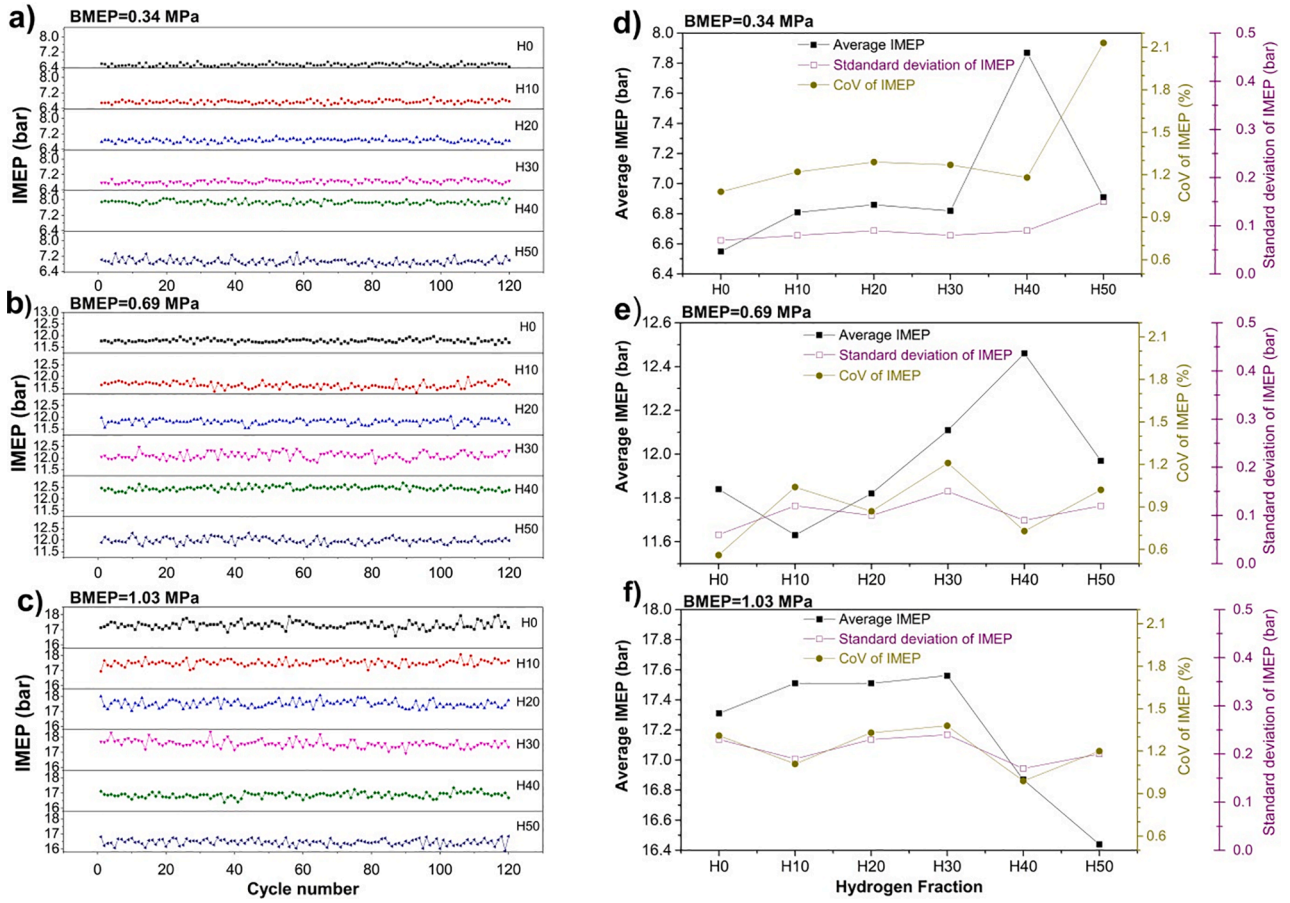

Fig. 9. Cyclic variations (a, b, and c) and average, standard deviation, and CoV (d, e, and f) of IMEP at different hydrogen fractions and BMEPs @1750 rpm.

range of about 0.3–0.4 MPa, but in this case the frequency remained in about 9–12 cycles (namely reduced the maximum repeatability) compared to that of the low load with and without hydrogen addition. This proved clearly an increase in the standard deviation of P_{max} at high load. This might be attributed to the more fuel amount supplied with the increased loads, and thus resulted in more various and greater values of the P_{max}, but in less repeatability.

3.3. Cyclic analysis of maximum pressure rise rate

The typical fluctuations of PRR_{max} for the consecutive 120 cycles, and average values, standard deviations, as well as COV of PRR_{max} under various hydrogen fractions and BMEPs are presented in Fig. 7 (a-f). The consecutive cyclic variations of the PRR_{max} were familiar with those of P_{max} as observed in Fig. 4. A small fraction of the hydrogen addition, as H10 and H20, reduced the average PRR_{max}, standard deviation, and CoV of PRR_{max} at medium and high BMEPs. However, more addition of the hydrogen increased the average PRR_{max} at all BMEPs in comparison with the diesel fuel operation, and this caused to slightly raise the combustion knock. It is required to keep the PRR_{max} under 5 bar/^{o}CA to obtain a low level of the combustion noise [35]. The highest average values of the PRR_{max} under various hydrogen fractions and test loads were found 4.1 bar/^{o}CA for H30 at low load, 4.15 bar/^{o}CA for H30 at medium load, and 5.63 bar/^{o}CA for H50 at high load. The results were within the acceptable PRR_{max} range, which meant that the severe knock was not detected [36]. As indicated in Fig. 7, as increasing the engine load, average PRR_{max} increased. The reason for that may be excursion in distribution of the air–fuel mixture, particularly at the start of ignition [29]. For all the test conditions, CoVs of PRR_{max} were in the range of 8.1–13.5%, which were considerably higher values when compared to those of P_{max}. It was principally caused from lower average PRR_{max} values [37]. On the other hand, the hydrogen addition was useful to decrease CoV of PRR_{max}, which was in accordance with the study performed by Zhou et al.[5]. As to the standard deviation of the PRR_{max}, it was following similar trend as CoV with respect to the hydrogen induction rate at a given load, and its value changed in the range of 0.3–0.74 bar/^{o}CA. It also increased with the increased engine load. Similar results were reported by Selim [29]. According to Selim [29], average combustion noise might be also reduced if the standard deviation of PRR_{max} was diminished.

Combustion noise is directly related to the magnitude of PRR_{max} and the location of PRR_{max}. High PRR_{max} values lead to undesirable effects on the mechanical durability of the engine. Fig. 8 depicts the values of the PRR_{max} and their corresponding locations (a, b, and c) for 720 data points, and frequency and distribution in the values of PRR_{max} (d, e, and f) under different hydrogen flow rates and BMEPs. From the Fig. 8 (a, b, and c), as increasing the engine load at a given hydrogen amount, locations of the PRR_{max} clearly concentrated in advanced CAs at the compression period, and the values of PRR_{max} increased. The earliest CA of PRR_{max} was 340° when the engine was operated at the BMEP of 1.03 MPa, and 76 cycles with different hydrogen fractions occurred at 340°CA. These were 24 cycles with H50, 22 cycles with H40, 14 cycles

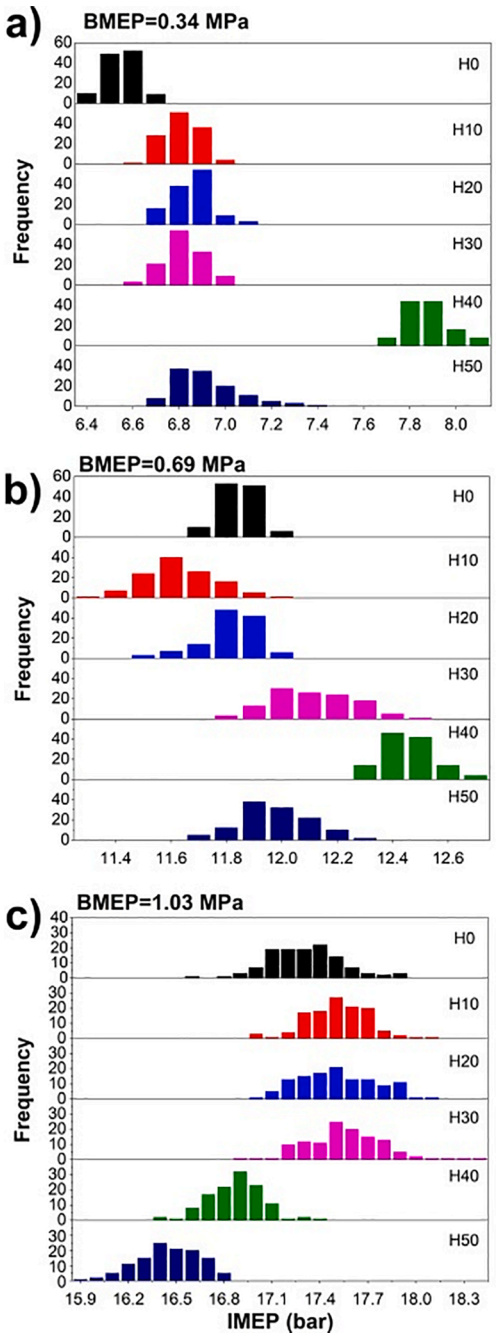

Fig. 10. Frequency of IMEP under different hydrogen fractions at different BMEPs @1750 rpm.

with diesel fuel, 9 cycles with H20, 5 cycles with H10, and 2 cycles with H30. As could be seen from the results, a larger addition of the hydrogen and increasing load led to move the PRR_{max} in the advanced CAs. However, some PRR_{max} points at middle and high loads occurred in retarded CAs, among 363–368°CAs. These tail-region points were frequently detected with the small amount of the hydrogen addition, which were H10 and H20. In the stages of pre- and main injection, the injection characteristics (amount, pressure, and timing etc.) of the pilot fuel can be slightly varied in each cycle [38]. This might cause a change in the ignition delay, particle size of the fuel, and duration of the initial flame development, which depends on leaner or richer mixture regions in the combustion chamber [39]. This allowed the PRR_{max} values to be produced at different CA positions. Similar results were reported in the study performed by Gupta and Mittal in a dual-fuel SI engine [18].

3.4. Cyclic analysis of indicated mean effective pressure

Fig. 9 depicts the typical fluctuations of IMEP at different BMEPs (a, b, and c) in 120 consecutive cycles, and average values, standard deviations, and CoVs of IMEP (d, e, and f) under all hydrogen addition levels and BMEPs. Compared to conventional diesel fuel, with larger hydrogen addition average IMEP increased at low and medium BMEPs, whereas decreased at high load. The largest increase in average IMEP was with H40 at low and medium loads, while with H30 at high load. It was clear that average IMEP increased with the engine load due to increasing the trapped mass. Larger supply of the main and pilot fuels at high load improved burning temperature and pressure; thus increased the combustion efficiency and IMEP. Regarding CoVs of IMEP, they were between 0.6 and 2.1%. The combustion was very stable because CoVs of IMEP were lower than 3%. [29,37,40,41,42]. Chintala and Subramanian [43] reported that CoV of IMEP was between 0.8 and 1.4% for various hydrogen fractions at different test conditions. They also remarked that CoVs of IMEP, PRR_{max}, and P_{max} were critical parameters and should be taken into consideration for determination of the knock tendency. If the combustion knock was able to be controlled, then more hydrogen proportion could be achieved in hydrogen-diesel fuelled CI engines. On the other hand, the enrichment of mixture with higher hydrogen ratios reduced the amount of the pilot diesel in the mixture. This could create larger homogeneous mixture regions in the combustion chamber, and thus providing significant decrease in CCVs of P_{max} and IMEP. The CoV trend of IMEP with hydrogen addition was similar to the standard deviation of IMEP, especially at medium and high loads. Moreover, it was observed that the standard deviation of the IMEP increased as the engine load increased. This could be expected since maximum and minimum values of the IMEP for 120 working cycles fluctuated in a wider range, as seen in Fig. 9 (b and c). If the difference between maximum and minimum IMEPs in consecutive cycles were decreased in each condition, then CCVs of IMEP could be reduced. Variation of the trapped charge mass in each cycle varied cyclic values of IMEP [8].

Frequency and distribution in the values of IMEP at different loads and hydrogen flow rates are presented in Fig. 10 (a-c). For the IMEP values, the concentrated distribution with the single diesel fuel was observed at low and medium loads, but there was a wider distribution at high load. As increasing the hydrogen amount, the values of IMEP were not only more distributed, but also their maximum repeatability was diminished at low and medium loads. Gaseous fuel utilization at high load was resulted in fast combustion period in premixed phase. More addition of the pilot fuel and hydrogen at high load was resulted in high temperature, and hence promoted robust burning rate. Instabilities in the fuel injection, variations in the ignition delay and the residual gas existence from previous cycle can intensely affect to cyclic variations. In addition, regional concentrations of the air waiting in the intake manifold during closed period of the intake valve may affect to the cyclic combustion. So, it could be seen cycle-to-cycle changes and different IMEP values in the subsequent working cycles in each operation case.

3.5. Cyclic analysis of mass fraction burned and combustion duration

Mass fraction burned is widely used parameter to obtain certain indications about the burning rate of mixture in the cylinder. In this study, MFB curve was determined by the Rassweiler-Withrow method [44]. In MFB figures, 0 refers to the start of combustion, while 1 refers to the end of combustion. Cyclic MFB variations with CA are compared at different hydrogen flow rates and loads in Fig. 11. Noticeably minimal cyclic MFB variations were found with the hydrogen-diesel operations under all

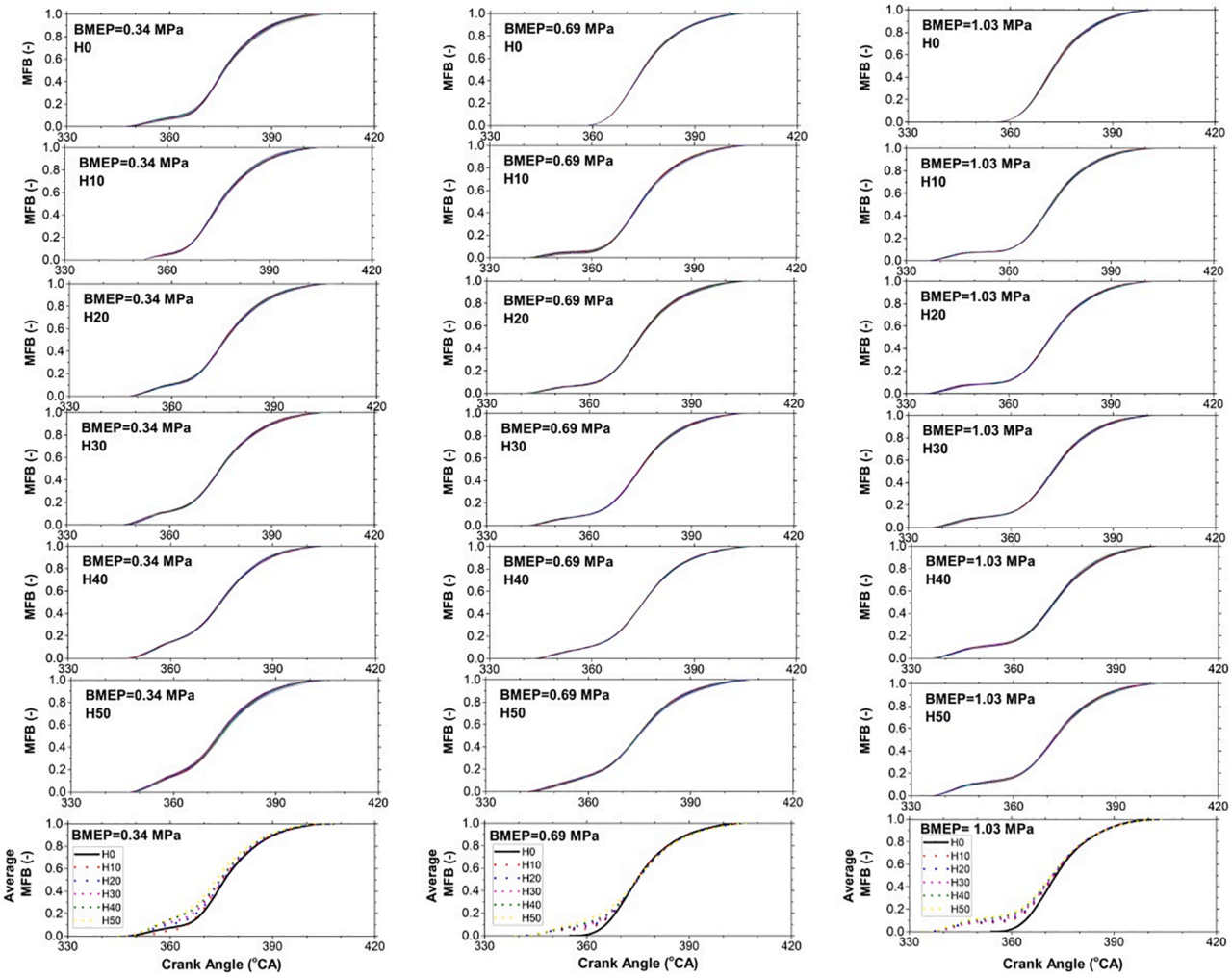

Fig. 11. Cycle-to-cycle variations of MFB for 120 cycles and their average with CA at different hydrogen fractions and BMEPs @1750 rpm.

BMEP conditions, and these findings were well consistent with the stable combustion pressure presented in Fig. 4. This implied that the stable burning for all conditions was maintained during 120 working cycles and the charge mass burned in each cycle became smoother. Wang et al. [19] reported greater cyclic MFB variations for different NG percentages in a CI engine owing to the nature of the used engine and fuel differences. It was observed in Fig. 11 that the start of combustion occurred before TDC. As an exception, the start of combustion of the standard diesel fuel operation was close to TDC at medium and high loads. It was clearly seen that the combustion of hydrogen-diesel engine basically started earlier when compared to single diesel fuel operation, and with increasing load the combustion was started at much earlier CAs. In previous combustion analyses done by the authors, this phenomenon was related to advanced pilot injection timing in dual-fuel operations depending on the engine load [25]. A similar trend of the average MFB curve was documented by Rao et al. [45] in a hydrogen enriched NG engine with variable spark timing; namely, a large fraction of the hydrogen addition caused faster burning of the mixture in a given CA. As different from the results presented here, Reyes et al. [46] reported significant CCVs in MFB in an SI engine without hydrogen addition, while cyclic MFB variations were decreased with hydrogen enrichment in NG dual-fuel engine. Similarly, Ceviz and Yüksel [47] reported highly large dispersion of cyclic MFB variations in an SI engine run with the liquified petroleum gas. It might be attributed to differences in the combustion process of the SI engine [29,47]. Oxidation of the fuel in the crevice region and near the cylinder wall became more unstable [24]. Consequently, this was resulted in larger CCVs of $MFB_{10\text{-}90}$. The average $MFB_{10\text{-}90}$ duration increased with the hydrogen addition at a constant BMEP, as seen in Fig. 12. For instance, $MFB_{10\text{-}90}$ durations at medium load of 0.69 MPa BMEP were 23.9, 26.2, 27.9, 29.6, 31.7, and 35.7°CA for the respective hydrogen flow rates of H0, H10, H20, H30, H40, and H50. CoV and standard deviation characteristics of $MFB_{10\text{-}90}$ were not obvious with the hydrogen addition. For $MFB_{10\text{-}90}$ duration, CoVs were in the range of 1.4–2.8% while the standard deviations were in the range of 0.35–0.9°CA. They were following with similar trend, as being in earlier combustion samples.

In Fig. 13 (a-c), the frequency and distribution in the values of $MFB_{10\text{-}90}$ for the 120 cycles are compared for different hydrogen flow rates and BMEP conditions. Approximate average of these distributions with respect to the hydrogen addition at a given BMEP was meanwhile noticed to be confirmed with net average values presented in Fig. 12. Remarkably, the diesel fuel test values at low BMEP distributed in a wider range in comparison with the hydrogen-diesel operations. However, at higher BMEP conditions it was observed that the distribution in the values of $MFB_{10\text{-}90}$ was more enlarged and resulted in the decreased frequency. The formation of different combustion durations during the 120 working cycles could be attributed to the occurrence of many ignition cores, variation of the turbulent movements, and variation of the amount of the residual gases. Hydrogen has higher flame speed and its fast flame propagation in the pre-mixed air–fuel mixture yields relatively stabilized combustion and shortens the burning duration for the diffusion combustion phase [5]. The existence of the residual gases

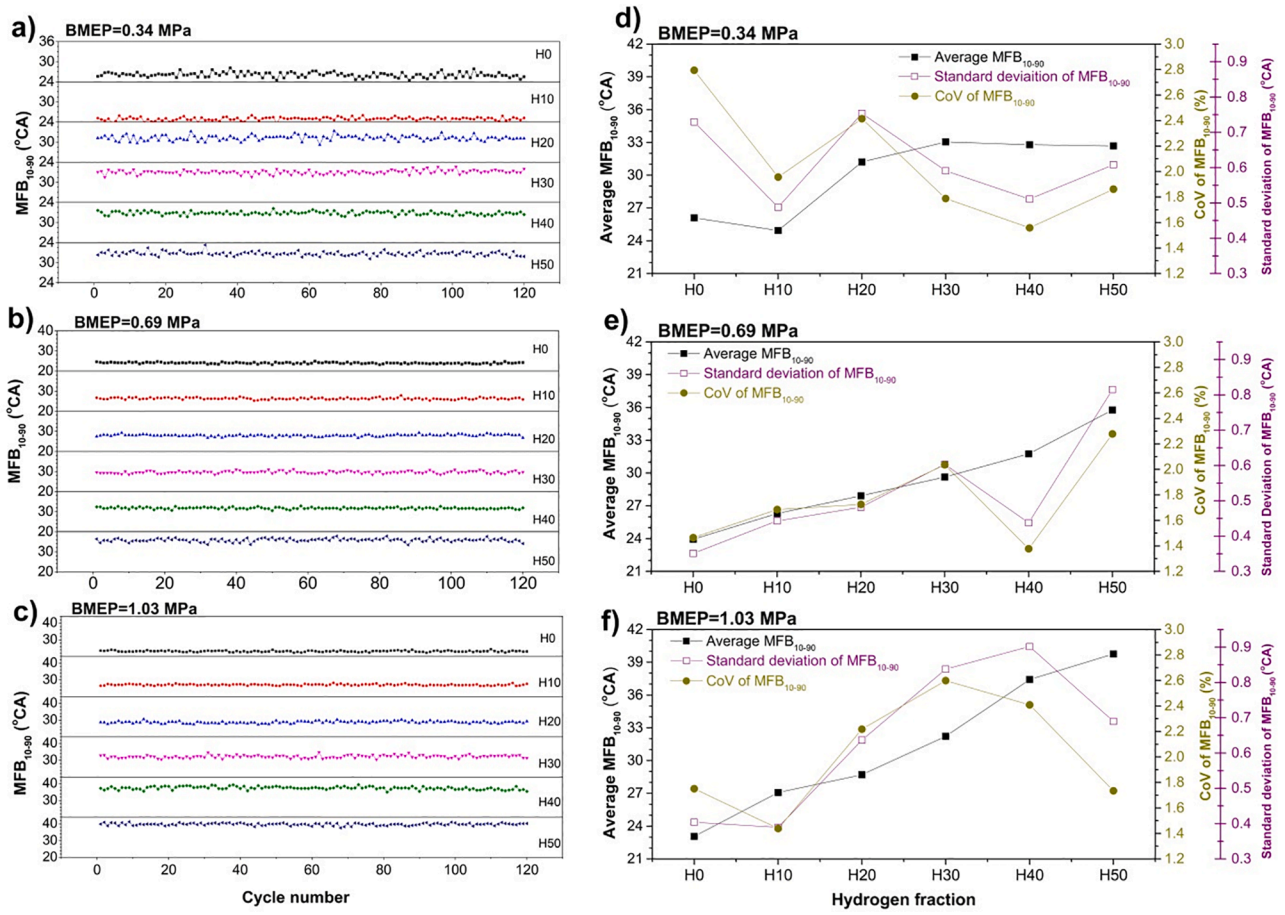

Fig. 12. Cyclic variations (a, b, and c), average, standard deviation, and CoV (d, e, and f) of MFB 10–90 duration under the different hydrogen fractions and BMEPs @1750 rpm.

in the combustion chamber, on the other hand, deteriorates the burning stabilization, and this opposite case can occur different combustion durations from cycle to cycle.

3.6. Correlation coefficients of the combustion parameters

In Fig. 14 (a-f), it was indicated variations of the correlation coefficients among P_{max}, PRR_{max}, IMEP, and MFB_{10-90} at different engine loads and hydrogen amounts in hydrogen-diesel fuelled CI engine. It is important to define relationship between major combustion parameters. Generally, absolute value of the correlation coefficient (R) less than 0.4 refers a weak linear correlation between the combustion parameters. If absolute R value is among 0.4–0.8 then it can be said to be obvious linear correlation between the combustion parameters [41]. It could be seen that there was a weak linear relationship between combustion parameters in most engine operations and hydrogen flow rates as seen in Fig. 14. Especially, R(IMEP, PRR_{max}), R(MFB_{10-90}, PRR_{max}), R(P_{max}, PRR_{max}), and R(MFB_{10-90}, IMEP) remained often under 0.4 value for the most cases, which could be meant that the these parameters were in weak relationship. On the other hand, R(IMEP, P_{max}), R(MFB_{10-90}, P_{max}), and R(MFB_{10-90}, IMEP) for some cases achieved over 0.4 as seen in Fig. 14 (c, e, and f), which implied that there was an obvious relation. The highest correlation coefficient between IMEP and P_{max} was respectively 0.55 and 0.6 for H50 at medium and high loads, and 0.45 and 0.49 between MFB_{10-90} and P_{max} for diesel fuel and H20 respectively at low load. In the literature, Turkcan [42], and Zhang et al. [48] showed a strong relation between IMEP and P_{max} in the ICEs fuelled with various alternative fuels under different loads. The variation of the R values between P_{max} and PRR_{max} was apparent with the engine load, and the correlation coefficient reduced with increased load. Furthermore, the effect of the hydrogen amount was less important for the most cases, as an except R(P_{max}, PRR_{max}) at only low load was decreased with increasing the hydrogen amount. On the contrary, Zhang et al.[48] found that the strongest correlation was between P_{max} and PRR_{max} rather than other combustion parameters for all test conditions in a NG fuelled SI engine. However, in this study R(MFB_{10-90}, IMEP), R(MFB_{10-90}, PRR_{max}), R(MFB_{10-90}, P_{max}), R(IMEP, P_{max}), and R(IMEP, PRR_{max}) were not dependant on changing the engine loads and hydrogen flow rates. Moreover, it was clearly observed that there was no negative value for R(IMEP, P_{max}) as illustrated in Fig. 14 (c) under the studied test loads and hydrogen amounts. Similarly, the correlation coefficients for all examined combustion parameters were not at all negative for the single diesel fuel at low load.

4. Conclusions

The impact of hydrogen addition on cycle-to-cycle variations in a common-rail, four-cylinder, four-stroke CI engine tested with different engine loads was experimentally studied. The main findings are as follows:

Stable combustion by comparing the combustion pressure and MFB traces with CA was found during consecutive combustion cycles, and there was not detected any pre-ignition cycle despite larger supplied hydrogen fractions. This was caused from continuing the lean-burn operations during the hydrogen-diesel operations. Compared to single diesel combustion, peak pressure of the hydrogen-diesel combustion augmented at only low load, whereas it diminished at medium and high loads. Moreover, the start of combustion was found earlier in hydrogen-

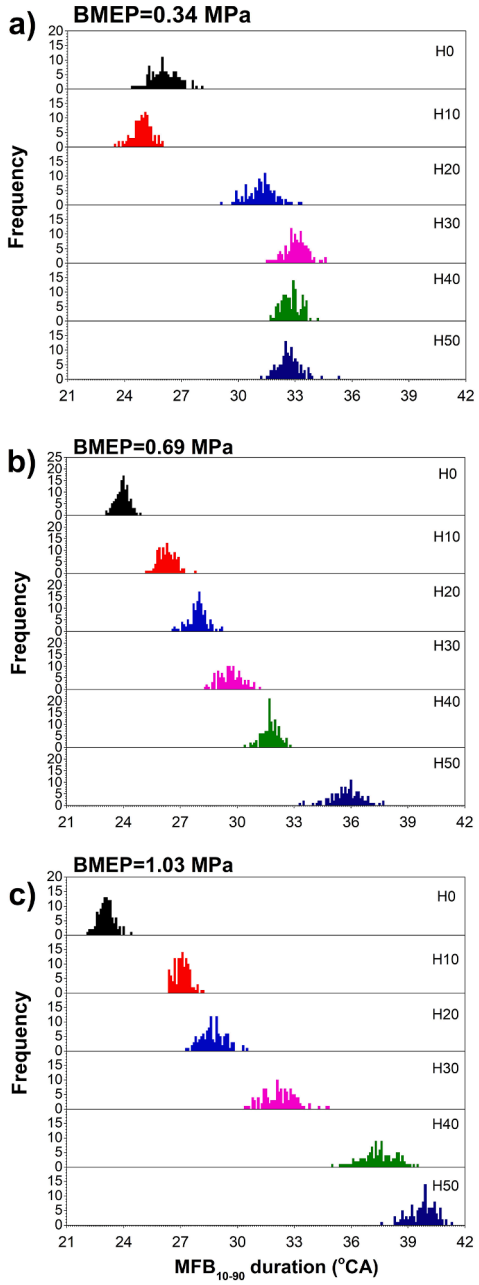

Fig. 13. Frequency distribution of $MFB_{10\text{-}90}$ duration with diesel and various hydrogen fractions at different BMEPs @1750 rpm.

diesel operations due to the advanced injection timing of the pilot diesel managed by the engine management system.

Overall effect of the hydrogen addition on the CCVs of IMEP, PRR_{max} and P_{max} was not obvious; however, for all of the hydrogen addition modes the combustion process was rather stable. CoV of IMEP, CoV of P_{max} and CoV of $MFB_{10\text{-}90}$ are all lower than 3%. As an except CoV of PRR_{max} was significantly higher as %8.1–13.5.

Standard deviation often followed similar trend as CoV. Its values changed in the range of 0.1–0.9 under all test conditions. The engine load was the most important factor for the standard deviation of the fundamental combustion parameters (P_{max}, PRR_{max}, and IMEP), namely the standard deviation of the mentioned combustion parameters increased with increase in engine load. The effect of hydrogen addition was not apparent for the inclination of the standard deviation and CoVs of the combustion parameters.

Frequencies of P_{max}, PRR_{max} and IMEP were moderate at low and medium loads whereas they were remarkably depleted at high load. Variety of values of P_{max}, PRR_{max} and IMEP was concentrated at low and medium loads but at high load it was distributed in a wider range; namely produced more values and therefore resulted in greater standard deviation.

There was a strong correlation between IMEP and P_{max} based on the computed R (correlation coefficient) values, especially with higher hydrogen introductions. Stable decreasing order for R(P_{max},PRR_{max}) became apparent at low load with the addition of hydrogen.

The overall results indicated that hydrogen addition was advisable

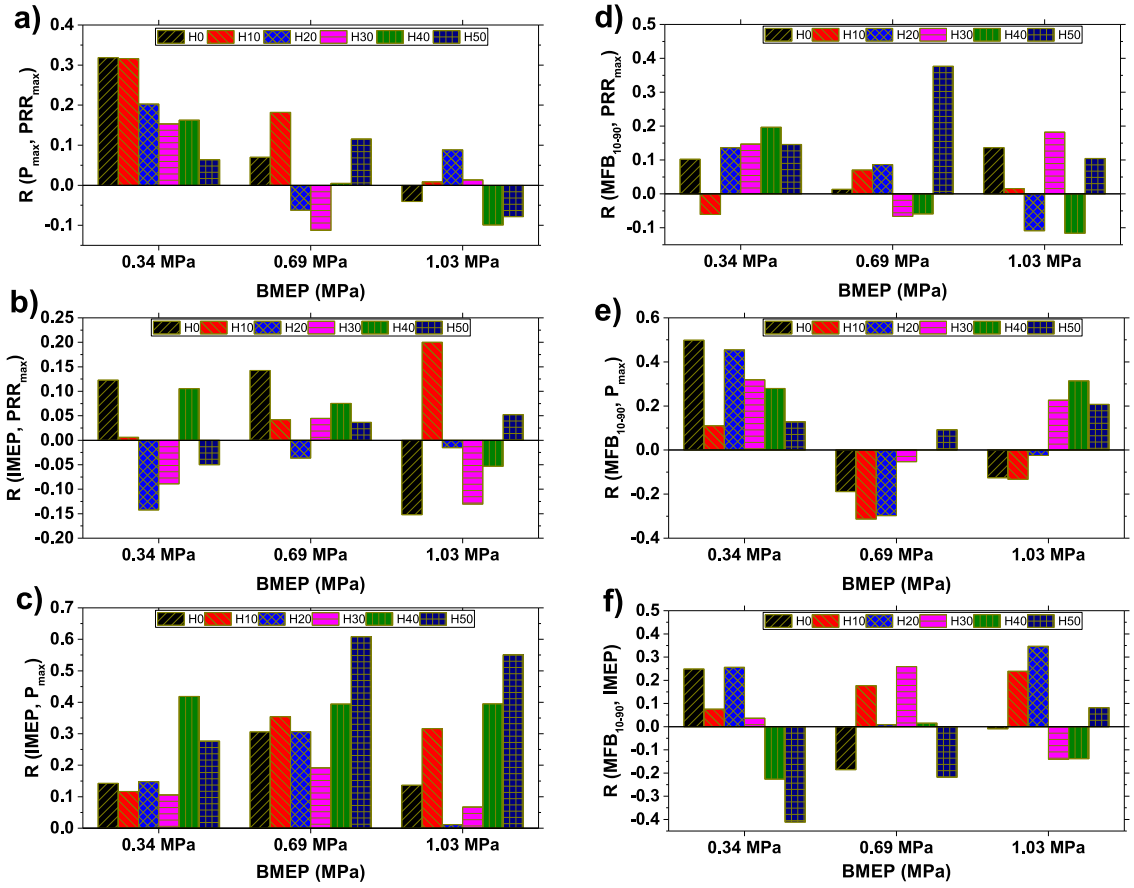

Fig. 14. Correlation coefficient between a) P_{max}&PRR_{max}, b)IMEP&PRR_{max}, c) IMEP&P_{max}, d) $MFB_{10\text{-}90}$&PRR_{max}, e) $MFB_{10\text{-}90}$&P_{max}, and f) $MFB_{10\text{-}90}$&IMEP @1750 rpm.

regarding cyclic variations for four-cylinder common-rail diesel engine operated at various engine loads.

CRediT authorship contribution statement

Ali Şanlı: Methodology, Investigation, Writing – review & editing, Writing – original draft. **İlker Turgut Yılmaz:** Writing – review & editing, Supervision.

Declaration of Competing Interest

The authors declare that they have no known competing financial interests or personal relationships that could have appeared to influence the work reported in this paper.

References

[1] Verhelst S. Recent progress in the use of hydrogen as a fuel for internal combustion engines. Int J Hydrog Energy 2014;39(2):1071–85. https://doi.org/10.1016/j.ijhydene.2013.10.102.
[2] Chintala V, Subramanian KA. A comprehensive review on utilization of hydrogen in a compression ignition engine under dual fuel mode. Renew Sust Energ Rev 2017;70:472–91. https://doi.org/10.1016/j.rser.2016.11.247.
[3] Kose H, Civiniz M. An experimental investigation of effect on diesel engine performance and exhaust emissions of addition at dual fuel mode of hydrogen. Fuel Process Technol 2013;114:26–34. https://doi.org/10.1016/j.fuproc.2013.03.023.
[4] Roy MM, Tomita E, Kawahara N, Harada Y, Sakane A. An experimental investigation on engine performance and emissions of a supercharged H_2-diesel dual-fuel engine. Int J Hydrog Energy 2010;35(2):844–53. https://doi.org/10.1016/j.ijhydene.2009.11.009.
[5] Zhou JH, Cheung CS, Zhao WZ, Leung CW. Diesel-hydrogen dual-fuel combustion and its impact on unregulated gaseous emissions and particulate emissions under different engine loads and engine speeds. Energy 2016;94:110–23. https://doi.org/10.1016/j.energy.2015.10.105.
[6] Jagadish C, Gumtapure V. Experimental studies on cyclic variations in a single cylinder diesel engine fuelled with raw biogas by dual mode of operation. Fuel 2020;266:117062. https://doi.org/10.1016/j.fuel.2020.117062.
[7] Kyrtatos P, Brücker C, Bouchoulos K. Cycle-to-cycle variations in diesel engines. Appl Energy 2016;171:120–32. https://doi.org/10.1016/j.apenergy.2016.03.015.
[8] Pera C, Chevillard S, Reveillon J. Effects of residual burnt gas heterogeneity on early flame propagation and on cyclic variability in spark-ignited engines. Combust Flame 2013;160(6):1020–32. https://doi.org/10.1016/j.combustflame.2013.01.009.
[9] Adomeit P, Lang O, Pishinger S, Aymanns R, Graf M, Stapf G. Analysis of cyclic fluctuations of charge motion and mixture formation in a DISI engine in stratified operation. SAE Tech Pap 2007;2007-01-1412. https://doi.org/10.4271/2007-01-1412.
[10] Sztenderowicz ML, Heywood JB. Mixture nonuniformity effects on S.I. engine combustion variability. SAE Tech Pap 1990;902142. https://doi.org/10.4271/902142.
[11] Maurya R, Agarwal A. Experimental investigation of cycle-by-cycle variations in CAI/HCCI combustion of gasoline and methanol fuelled engine. SAE Tech Pap 2009;2009-01-1345. https://doi.org/10.4271/2009-01-1345.
[12] Deng B, Hou K, Duan X, Xu Z. The correlation between intake fluctuation and combustion CCv (Cycle-to-cycle variations) on a high speed gasoline engine: A wide range operating condition study. Fuel 2021;304:121336. https://doi.org/10.1016/j.fuel.2021.121336.
[13] Yang L, Zare A, Bodisco TA, Nabi N, Liu Z, Brown RJ. Analysis of cycle-to-cycle variations in a common-rail compression ignition engine fuelled with diesel and biodiesel fuels. Fuel 2021;290:120010. https://doi.org/10.1016/j.fuel.2020.120010.
[14] Ceviz MA, Çavuşoğlu B, Kaya F, Öner İV. Determination of cycle number for real in-cylinder pressure cycle analysis in internal combustion engines. Energy 2011;36:2465–72. https://doi.org/10.1016/j.energy.2011.01.038.
[15] Santoso WB, Bakar RA, Ariyono S, Cholis N. Study of cyclic variability in diesel-hydrogen dual fuel engine combustion. Int J Mech Mech Eng 2012;12(4):52–6.
[16] Wang Y, Xiao F, Zhao Y, Li D, Lei X. Study on cycle-by-cycle variations in a diesel engine with dimethyl ether as port premixing fuel. Appl Energy 2015;143:58–70. https://doi.org/10.1016/j.apenergy.2014.12.079.

[17] Zheng J, Huang Z, Wang J, Wang B, Ning D, Zhang Y. Effect of compression ratio on cycle-by-cycle variations in a natural gas direct injection engine. Energy Fuels 2009;23(11):5357–66. https://doi.org/10.1021/ef900651p.
[18] Gupta SK, Mittal M. Analysis of Cycle-to-cycle combustion variations in a spark-ignition engine operating under various biogas compositions. Energy Fuels 2019; 33:12421–30. https://doi.org/10.1021/acs.energyfuels.9b02344.
[19] Wang Z, Fu W, Wang D, Xu Y, Du G, You J. A multilevel study on the influence of natural gas substitution rate on combustion and cyclic variation in a diesel/natural gas dual fuel engine. Fuel 2021;294:120499. https://doi.org/10.1016/j.fuel.2021.120499.
[20] Jha PR, Krishnan SR, Srinivasan KK. Impact of methane energy fraction on emissions, performance and cyclic variability in low-load dual fuel combustion at early injection timings. Int J Engine Res 2019;22(4):1255–72. https://doi.org/10.1177/1468087419892380.
[21] Chen Z, He J, Chen H, Geng H, Geng L, Zhang P. Experimental study on the cycle-to-cycle variations in natural gas/methanol bi-fueled engine under excess air/fuel ratio at 1.6. Energy 2021;224:120233. https://doi.org/10.1016/j.energy.2021.120233.
[22] Chen Z, Chen H, Geng L. Influence of water port injection on cycle-to-cycle variations in heavy-duty natural gas engine under low load. Fuel 2020;280: 118678. https://doi.org/10.1016/j.fuel.2020.118678.
[23] Ma F, Wang Y, Liu H, Li Y, Wang J, Ding S. Effects of hydrogen addition on cycle-by-cycle variations in a lean burn natural gas spark-ignition engine. Int J Hydrog Energy 2008;33(2):823–31. https://doi.org/10.1016/j.ijhydene.2007.10.043.
[24] Duan X, Deng B, Liu Y, Zou S, Liu J, Feng R. An experimental study the impact of the hydrogen enrichment on cycle-to-cycle variations of the large bore and lean burn natural gas spark-ignition engine. Fuel 2020;282:118868. https://doi.org/10.1016/j.fuel.2020.118868.
[25] Sanli A, Yilmaz IT, Gumus M. Investigation of combustion and emissions characteristics in a TBC diesel engine fuelled with CH_4-CO_2-H_2 mixtures. Int J Hydrog Energy 2021;46(47):24395–404. https://doi.org/10.1016/j.ijhydene.2021.05.014.
[26] Yilmaz IT. The effect of hydrogen on the thermal efficiency and combustion process of the low compression ratio CI engine. App Thermal Eng 2021;197: 117381. https://doi.org/10.1016/j.applthermaleng.2021.117381.
[27] Gong C, Huang K, Chen Y, Jia J, Su Y, Liu X. Cycle-by-cycle combustion variation in a DISI engine fueled with methanol. Fuel 2011;90:2817–9. https://doi.org/10.1016/j.fuel.2011.04.010.
[28] Nag S, Dhar A, Gupta A. Hydrogen-diesel co-combustion characteristics, vibro-acoustics and regulated emissions in EGR assisted dual fuel engine. Fuel 2022;307: 121925. https://doi.org/10.1016/j.fuel.2021.121925.
[29] Selim MYE. Effect of engine parameters and gaseous fuel type on the cyclic variability of dual fuel engines. Fuel 2005;84(7–8):961–71. https://doi.org/10.1016/j.fuel.2004.11.023.
[30] Li GX, Yao BF. Nonlinear dynamics of cycle-to-cycle combustion variations in a lean-burn natural gas engine. Appl Therm Eng 2008;28:611–20. https://doi.org/10.1016/j.applthermaleng.2007.04.008.
[31] Heywood JB. Internal combustion engine fundamentals. New York: McGraw-Hill Book Company; 1988.
[32] Zhang M, Hong W, Xie F, Liu Y, Su Y, Li X, et al. Effects of diluents on cycle-by-cycle variations in a spark ignition engine fueled with methanol. Energy 2019;182: 1132–40. https://doi.org/10.1016/j.energy.2019.06.110.
[33] Wang J, Huang Z, Miao H, Wang X, Jiang D. Study of cyclic variations of direct-injection combustion fuelled with natural gas-hydrogen blends using a constant volume vessel. Int J Hydrog Energy 2008;33(24):7580–91. https://doi.org/10.1016/j.ijhydene.2008.09.041.
[34] Gupta SK, Mittal M. Effect of compression ratio on the performance and emission characteristics, and cycle-to-cycle combustion variations of a spark-ignition engine fuelled with bio-methane surrogate. Appl Therm Eng 2019;148:1440–53. https://doi.org/10.1016/j.applthermaleng.2018.11.057.
[35] Miyamoto T, Hasegawa H, Mikami M, Kojima N, Kabashima H, Urata Y. Effect of hydrogen addition to intake gas on combustion and exhaust emission characteristics of a diesel engine. Int J Hydrog Energy 2011;36(20):13138–49. https://doi.org/10.1016/j.ijhydene.2011.06.144.
[36] Cheng Q, Ahmad Z, Kaario O, Vuorinen V, Larmi M. Experimental study on tri-fuel combustion using premixed methane-hydrogen mixtures ignited by a diesel pilot. Int J Hydrog Energy 2021;46(40):21182–97. https://doi.org/10.1016/j.ijhydene.2021.03.215.
[37] Gürbüz H, Akçay İH, Buran D. An investigation on effect of in-cylinder swirl flow on performance, combustion and cyclic variations in hydrogen fuelled spark ignition engine. J Energy Ins 2014;87:1–10. https://doi.org/10.1016/j.joei.2012.03.001.
[38] Zhong L, Singh IP, Han J, Lai M-C, Henein NA. Effects of cycle-to-cycle variation in the injection pressure in a common rail diesel injection system on engine performance. SAE Tech Pap 2003;2003-01-0699. https://doi.org/10.4271/2003-01-0699.
[39] Sanli A, Yilmaz IT, Gumus M. Experimental evaluation of performance and combustion characteristics in a hydrogen-methane port fuelled diesel engine at different compression ratios. Energy Fuels 2020;34:2272–83. https://doi.org/10.1021/acs.energyfuels.9b03033.
[40] Wu HW, Wu ZY. Investigation on combustion characteristics and emissions of diesel/hydrogen mixtures by using energy-share method in a diesel engine. Appl Therm Eng 2021;42:154–62. https://doi.org/10.1016/j.applthermaleng.2012.03.004.
[41] Jamrozik A, Rogalinski KG, Tutak W. Hydrogen effects on combustion stability, performance and emission of diesel engine. Int J Hydrog Energy 2020;45(38): 19936–47. https://doi.org/10.1016/j.ijhydene.2020.05.049.
[42] Turkcan A. The effects of different types of biodiesels and biodiesel-bioethanol-diesel blends on the cyclic variations and correlation coefficient. Fuel 2020;261: 116453. https://doi.org/10.1016/j.fuel.2019.116453.
[43] Chintala V, Subramanian KA. An effort to enhance hydrogen energy share in a compression ignition engine under dual-fuel mode using low temperature combustion strategies. Appl Energy 2015;146:174–83. https://doi.org/10.1016/j.apenergy.2015.01.110.
[44] Rassweiler GM, Withrow L. Motion pictures of engine flames correlated with pressure cards. SAE Tech Pap 1938;380139. https://doi.org/10.4271/380139.
[45] Rao A, Wu Z, Mehra RK, Duan H, Ma F. Effect of hydrogen addition on combustion, performance and emission of stoichiometric compressed natural gas fuelled internal combustion engine along with exhaust gas recirculation at low, half and high load conditions. Fuel 2021;304:121358. https://doi.org/10.1016/j.fuel.2021.121358.
[46] Reyes M, Tinaut FV, Melgar A, Perez A. Characterization of the combustion process and cycle-to-cycle variations in a spark ignition engine fuelled with natural gas/hydrogen mixtures. Int J Hydrog Energy 2016;41(3):2064–74. https://doi.org/10.1016/j.ijhydene.2015.10.082.
[47] Ceviz MA, Yüksel F. Cyclic variations on LPG and gasoline-fuelled lean burn SI engine. Renew Energy 2006;31(12):1950–60. https://doi.org/10.1016/j.renene.2005.09.016.
[48] Zhang HG, Han XJ, Yao BF, Li GX. Study on the effect of engine operation parameters on cyclic combustion variations and correlation coefficient between the pressure-related parameters of a CNG engine. Appl Energy 2013;104:992–1002. https://doi.org/10.1016/j.apenergy.2012.11.043.